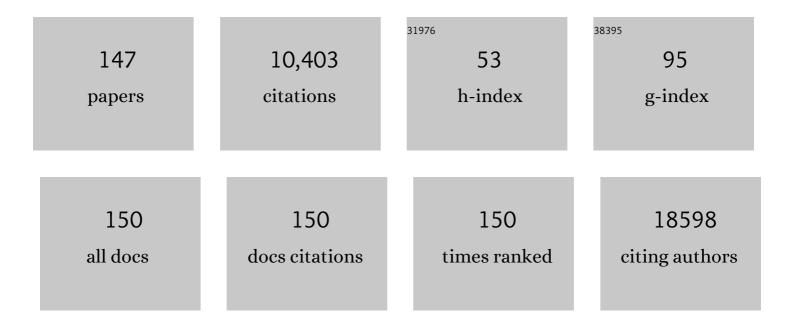
## Katrina M Waters

List of Publications by Year in descending order

Source: https://exaly.com/author-pdf/9429669/publications.pdf Version: 2024-02-01



#	Article	IF	CITATIONS
1	Sharing and community curation of mass spectrometry data with Global Natural Products Social Molecular Networking. Nature Biotechnology, 2016, 34, 828-837.	17.5	2,802
2	Temporal Proteome and Lipidome Profiles Reveal Hepatitis C Virus-Associated Reprogramming of Hepatocellular Metabolism and Bioenergetics. PLoS Pathogens, 2010, 6, e1000719.	4.7	361
3	Mechanisms of Severe Acute Respiratory Syndrome Coronavirus-Induced Acute Lung Injury. MBio, 2013, 4, .	4.1	251
4	Pathogenic Influenza Viruses and Coronaviruses Utilize Similar and Contrasting Approaches To Control Interferon-Stimulated Gene Responses. MBio, 2014, 5, e01174-14.	4.1	246
5	Review, Evaluation, and Discussion of the Challenges of Missing Value Imputation for Mass Spectrometry-Based Label-Free Global Proteomics. Journal of Proteome Research, 2015, 14, 1993-2001.	3.7	217
6	Macrophage Responses to Silica Nanoparticles are Highly Conserved Across Particle Sizes. Toxicological Sciences, 2009, 107, 553-569.	3.1	207
7	MARRVEL: Integration of Human and Model Organism Genetic Resources to Facilitate Functional Annotation of the Human Genome. American Journal of Human Genetics, 2017, 100, 843-853.	6.2	181
8	Comparative developmental toxicity of environmentally relevant oxygenated PAHs. Toxicology and Applied Pharmacology, 2013, 271, 266-275.	2.8	164
9	The Undiagnosed Diseases Network: Accelerating Discovery about Health and Disease. American Journal of Human Genetics, 2017, 100, 185-192.	6.2	142
10	MERS-CoV and H5N1 influenza virus antagonize antigen presentation by altering the epigenetic landscape. Proceedings of the National Academy of Sciences of the United States of America, 2018, 115, E1012-E1021.	7.1	142
11	Polycyclic aromatic hydrocarbons as skin carcinogens: Comparison of benzo[a]pyrene, dibenzo[def,p]chrysene and three environmental mixtures in the FVB/N mouse. Toxicology and Applied Pharmacology, 2012, 264, 377-386.	2.8	140
12	Release of Severe Acute Respiratory Syndrome Coronavirus Nuclear Import Block Enhances Host Transcription in Human Lung Cells. Journal of Virology, 2013, 87, 3885-3902.	3.4	140
13	MERS-CoV Accessory ORFs Play Key Role for Infection and Pathogenesis. MBio, 2017, 8, .	4.1	126
14	How Adverse Outcome Pathways Can Aid the Development and Use of Computational Prediction Models for Regulatory Toxicology. Toxicological Sciences, 2017, 155, 326-336.	3.1	125
15	Differential Gene Expression in Response to Methoxychlor and Estradiol through ERalpha, ERbeta, and AR in Reproductive Tissues of Female Mice. Toxicological Sciences, 2001, 63, 47-56.	3.1	119
16	Investigating the correspondence between transcriptomic and proteomic expression profiles using coupled cluster models. Bioinformatics, 2008, 24, 2894-2900.	4.1	117
17	Insulin and dietary fructose induce stearoyl-CoA desaturase 1 gene expression of diabetic mice Journal of Biological Chemistry, 1994, 269, 27773-27777.	3.4	109
18	Comparative Proteomics and Pulmonary Toxicity of Instilled Single-Walled Carbon Nanotubes, Crocidolite Aspestos, and Ultrafine Carbon Black in Mice, Toxicological Sciences, 2011, 120, 123-135	3.1	103

#	Article	IF	CITATIONS
19	Completing the Link between Exposure Science and Toxicology for Improved Environmental Health Decision Making: The Aggregate Exposure Pathway Framework. Environmental Science & Technology, 2016, 50, 4579-4586.	10.0	96
20	A Syndromic Neurodevelopmental Disorder Caused by De Novo Variants in EBF3. American Journal of Human Genetics, 2017, 100, 128-137.	6.2	96
21	Data merging for integrated microarray and proteomic analysis. Briefings in Functional Genomics & Proteomics, 2006, 5, 261-272.	3.8	95
22	Combined Statistical Analyses of Peptide Intensities and Peptide Occurrences Improves Identification of Significant Peptides from MS-Based Proteomics Data. Journal of Proteome Research, 2010, 9, 5748-5756.	3.7	93
23	Middle East Respiratory Syndrome Coronavirus Nonstructural Protein 16 Is Necessary for Interferon Resistance and Viral Pathogenesis. MSphere, 2017, 2, .	2.9	92
24	Insulin and dietary fructose induce stearoyl-CoA desaturase 1 gene expression of diabetic mice. Journal of Biological Chemistry, 1994, 269, 27773-7.	3.4	89
25	Improved quality control processing of peptide-centric LC-MS proteomics data. Bioinformatics, 2011, 27, 2866-2872.	4.1	88
26	Multi-platform 'Omics Analysis of Human Ebola Virus Disease Pathogenesis. Cell Host and Microbe, 2017, 22, 817-829.e8.	11.0	88
27	Silicone wristbands compared with traditional polycyclic aromatic hydrocarbon exposure assessment methods. Analytical and Bioanalytical Chemistry, 2018, 410, 3059-3071.	3.7	85
28	A statistical selection strategy for normalization procedures in LCâ€MS proteomics experiments through datasetâ€dependent ranking of normalization scaling factors. Proteomics, 2011, 11, 4736-4741.	2.2	82
29	Implications of Bioremediation of Polycyclic Aromatic Hydrocarbon-Contaminated Soils for Human Health and Cancer Risk. Environmental Science & Technology, 2017, 51, 9458-9468.	10.0	82
30	Estrogen Regulation of a Transforming Growth Factor-Î <sup>2</sup> Inducible Early Gene That Inhibits Deoxyribonucleic Acid Synthesis in Human Osteoblasts*. Endocrinology, 1998, 139, 1346-1353.	2.8	78
31	Host Regulatory Network Response to Infection with Highly Pathogenic H5N1 Avian Influenza Virus. Journal of Virology, 2011, 85, 10955-10967.	3.4	77
32	AHR2 Mutant Reveals Functional Diversity of Aryl Hydrocarbon Receptors in Zebrafish. PLoS ONE, 2012, 7, e29346.	2.5	77
33	Estrogen regulation of human osteoblast function is determined by the stage of differentiation and the estrogen receptor isoform. Journal of Cellular Biochemistry, 2001, 83, 448-462.	2.6	75
34	Integrated Omics Analysis of Pathogenic Host Responses during Pandemic H1N1 Influenza Virus Infection: The Crucial Role of Lipid Metabolism. Cell Host and Microbe, 2016, 19, 254-266.	11.0	75
35	MicroRNAs control neurobehavioral development and function in zebrafish. FASEB Journal, 2012, 26, 1452-1461.	0.5	74
36	A comparative analysis of computational approaches to relative protein quantification using peptide peak intensities in labelâ€free <scp>LC</scp> â€ <scp>MS</scp> proteomics experiments. Proteomics, 2013, 13, 493-503.	2.2	74

#	Article	IF	CITATIONS
37	Structurally distinct polycyclic aromatic hydrocarbons induce differential transcriptional responses in developing zebrafish. Toxicology and Applied Pharmacology, 2013, 272, 656-670.	2.8	73
38	Overexpression of a Nuclear Protein, TIEG, Mimics Transforming Growth Factor-Î <sup>2</sup> Action in Human Osteoblast Cells. Journal of Biological Chemistry, 2000, 275, 20255-20259.	3.4	72
39	lon mobility spectrometry and the omics: Distinguishing isomers, molecular classes and contaminant ions in complex samples. TrAC - Trends in Analytical Chemistry, 2019, 116, 292-299.	11.4	71
40	Discovery of Novel Glucose-Regulated Proteins in Isolated Human Pancreatic Islets Using LC–MS/MS-Based Proteomics. Journal of Proteome Research, 2012, 11, 3520-3532.	3.7	69
41	IRF2BPL Is Associated with Neurological Phenotypes. American Journal of Human Genetics, 2018, 103, 245-260.	6.2	69
42	A Network Integration Approach to Predict Conserved Regulators Related to Pathogenicity of Influenza and SARS-CoV Respiratory Viruses. PLoS ONE, 2013, 8, e69374.	2.5	68
43	Surface functionalities of gold nanoparticles impact embryonic gene expression responses. Nanotoxicology, 2013, 7, 192-201.	3.0	64
44	A comprehensive collection of systems biology data characterizing the host response to viral infection. Scientific Data, 2014, 1, 140033.	5.3	62
45	Plasma lipidome reveals critical illness and recovery from human Ebola virus disease. Proceedings of the United States of America, 2019, 116, 3919-3928.	7.1	62
46	A comprehensive iterative approach is highly effective in diagnosing individuals who are exome negative. Genetics in Medicine, 2019, 21, 161-172.	2.4	60
47	A support vector machine model for the prediction of proteotypic peptides for accurate mass and time proteomics. Bioinformatics, 2008, 24, 1503-1509.	4.1	59
48	Three human cell types respond to multi-walled carbon nanotubes and titanium dioxide nanobelts with cell-specific transcriptomic and proteomic expression patterns. Nanotoxicology, 2014, 8, 533-548.	3.0	59
49	Biallelic Mutations in ATP5F1D, which Encodes a Subunit of ATP Synthase, Cause a Metabolic Disorder. American Journal of Human Genetics, 2018, 102, 494-504.	6.2	59
50	Expanding the Spectrum of BAF-Related Disorders: De Novo Variants in SMARCC2 Cause a Syndrome with Intellectual Disability and Developmental Delay. American Journal of Human Genetics, 2019, 104, 164-178.	6.2	59
51	Regulation of Hepatic Stearoyl-CoA Desaturase Gene 1 by Vitamin A. Biochemical and Biophysical Research Communications, 1997, 231, 206-210.	2.1	58
52	The effect of inhibition of PP1 and TNFα signaling on pathogenesis of SARS coronavirus. BMC Systems Biology, 2016, 10, 93.	3.0	58
53	Combination Attenuation Offers Strategy for Live Attenuated Coronavirus Vaccines. Journal of Virology, 2018, 92, .	3.4	58
54	Localization of a polyunsaturated fatty acid response region in stearoyl-CoA desaturase gene 1. Lipids and Lipid Metabolism, 1997, 1349, 33-42.	2.6	56

#	Article	IF	CITATIONS
55	Discovery of common chemical exposures across three continents using silicone wristbands. Royal Society Open Science, 2019, 6, 181836.	2.4	56
56	Polyunsaturated fatty acids inhibit hepatic stearoyl-CoA desaturase-1 gene in diabetic mice. Lipids, 1996, 31, S33-S36.	1.7	54
57	Ligand-Specific Transcriptional Mechanisms Underlie Aryl Hydrocarbon Receptor-Mediated Developmental Toxicity of Oxygenated PAHs. Toxicological Sciences, 2015, 147, 397-411.	3.1	54
58	Silymarin Suppresses Cellular Inflammation By Inducing Reparative Stress Signaling. Journal of Natural Products, 2015, 78, 1990-2000.	3.0	53
59	Topological analysis of protein co-abundance networks identifies novel host targets important for HCV infection and pathogenesis. BMC Systems Biology, 2012, 6, 28.	3.0	52
60	Comparative iron oxide nanoparticle cellular dosimetry and response in mice by the inhalation and liquid cell culture exposure routes. Particle and Fibre Toxicology, 2014, 11, 46.	6.2	49
61	Systems Virology Identifies a Mitochondrial Fatty Acid Oxidation Enzyme, Dodecenoyl Coenzyme A Delta Isomerase, Required for Hepatitis C Virus Replication and Likely Pathogenesis. Journal of Virology, 2011, 85, 11646-11654.	3.4	48
62	Enabling high-throughput data management for systems biology: The Bioinformatics Resource Manager. Bioinformatics, 2007, 23, 906-909.	4.1	45
63	Phenotypically anchored transcriptome profiling of developmental exposure to the antimicrobial agent, triclosan, reveals hepatotoxicity in embryonic zebrafish. Toxicology and Applied Pharmacology, 2016, 308, 32-45.	2.8	45
64	MPLEx: a method for simultaneous pathogen inactivation and extraction of samples for multi-omics profiling. Analyst, The, 2017, 142, 442-448.	3.5	43
65	Relative Influence of Trans-Pacific and Regional Atmospheric Transport of PAHs in the Pacific Northwest, U.S Environmental Science & Technology, 2015, 49, 13807-13816.	10.0	42
66	Estrogen Receptor Isoform-Specific Induction of Progesterone Receptors in Human Osteoblasts. Journal of Bone and Mineral Research, 2002, 17, 580-592.	2.8	41
67	Conserved host response to highly pathogenic avian influenza virus infection in human cell culture, mouse and macaque model systems. BMC Systems Biology, 2011, 5, 190.	3.0	41
68	A support vector machine model for the prediction of proteotypic peptides for accurate mass and time proteomics. Bioinformatics, 2010, 26, 1677-1683.	4.1	39
69	Proteome and computational analyses reveal new insights into the mechanisms of hepatitis C virus-mediated liver disease posttransplantation. Hepatology, 2012, 56, 28-38.	7.3	39
70	Global gene expression analysis reveals pathway differences between teratogenic and non-teratogenic exposure concentrations of bisphenol A and 171²-estradiol in embryonic zebrafish. Reproductive Toxicology, 2013, 38, 89-101.	2.9	39
71	Coupling Genome-wide Transcriptomics and Developmental Toxicity Profiles in Zebrafish to Characterize Polycyclic Aromatic Hydrocarbon (PAH) Hazard. International Journal of Molecular Sciences, 2019, 20, 2570.	4.1	39
72	<i>pmartR</i> : Quality Control and Statistics for Mass Spectrometry-Based Biological Data. Journal of Proteome Research, 2019, 18, 1418-1425.	3.7	39

#	Article	IF	CITATIONS
73	Hypergraph models of biological networks to identify genes critical to pathogenic viral response. BMC Bioinformatics, 2021, 22, 287.	2.6	39
74	Bayesian Proteoform Modeling Improves Protein Quantification of Global Proteomic Measurements. Molecular and Cellular Proteomics, 2014, 13, 3639-3646.	3.8	38
75	Network Analysis of Epidermal Growth Factor Signaling Using Integrated Genomic, Proteomic and Phosphorylation Data. PLoS ONE, 2012, 7, e34515.	2.5	37
76	Association of Carcinogenic Polycyclic Aromatic Hydrocarbon Emissions and Smoking with Lung Cancer Mortality Rates on a Global Scale. Environmental Science & Technology, 2013, 47, 3410-3416.	10.0	36
77	A Recurrent De Novo Variant in NACC1 Causes a Syndrome Characterized by Infantile Epilepsy, Cataracts, and Profound Developmental Delay. American Journal of Human Genetics, 2017, 100, 343-351.	6.2	35
78	Localization of a Negative Thyroid Hormone-Response Region in Hepatic Stearoyl-CoA Desaturase Gene 1. Biochemical and Biophysical Research Communications, 1997, 233, 838-843.	2.1	34
79	Effect of Native American Fish Smoking Methods on Dietary Exposure to Polycyclic Aromatic Hydrocarbons and Possible Risks to Human Health. Journal of Agricultural and Food Chemistry, 2012, 60, 6899-6906.	5.2	34
80	Bone Growth and Turnover in Progesterone Receptor Knockout Mice. Endocrinology, 2008, 149, 2383-2390.	2.8	33
81	Controlling the Response: Predictive Modeling of a Highly Central, Pathogen-Targeted Core Response Module in Macrophage Activation. PLoS ONE, 2011, 6, e14673.	2.5	33
82	Direct Action of Naturally Occurring Estrogen Metabolites on Human Osteoblastic Cells. Journal of Bone and Mineral Research, 2010, 15, 499-506.	2.8	30
83	Identifying efficacious approaches to chemoprevention with chlorophyllin, purified chlorophylls and freeze-dried spinach in a mouse model of transplacental carcinogenesis. Carcinogenesis, 2008, 30, 315-320.	2.8	29
84	The Mammary Epithelial Cell Secretome and Its Regulation by Signal Transduction Pathways. Journal of Proteome Research, 2008, 7, 558-569.	3.7	29
85	Integrative transcriptomic and proteomic analysis of osteocytic cells exposed to fluid flow reveals novel mechano-sensitive signaling pathways. Journal of Biomechanics, 2014, 47, 1838-1845.	2.1	29
86	Transplacental carcinogenesis with dibenzo[def,p]chrysene (DBC): Timing of maternal exposures determines target tissue response in offspring. Cancer Letters, 2012, 317, 49-55.	7.2	28
87	A statistical analysis of the effects of urease pre-treatment on the measurement of the urinary metabolome by gas chromatography–mass spectrometry. Metabolomics, 2014, 10, 897-908.	3.0	28
88	Bi-allelic Variants in TONSL Cause SPONASTRIME Dysplasia and a Spectrum of Skeletal Dysplasia Phenotypes. American Journal of Human Genetics, 2019, 104, 422-438.	6.2	27
89	Cytochrome P450 1b1 in polycyclic aromatic hydrocarbon (PAH)-induced skin carcinogenesis: Tumorigenicity of individual PAHs and coal-tar extract, DNA adduction and expression of select genes in the Cyp1b1 knockout mouse. Toxicology and Applied Pharmacology, 2015, 287, 149-160.	2.8	26
90	Annexin A2 Modulates Radiation-Sensitive Transcriptional Programming and Cell Fate. Radiation Research, 2013, 179, 53-61.	1.5	23

#	Article	IF	CITATIONS
91	Mechanism-Based Classification of PAH Mixtures to Predict Carcinogenic Potential. Toxicological Sciences, 2015, 146, 135-145.	3.1	23
92	Transcriptomic and phenotypic profiling in developing zebrafish exposed to thyroid hormone receptor agonists. Reproductive Toxicology, 2018, 77, 80-93.	2.9	23
93	Indoor versus Outdoor Air Quality during Wildfires. Environmental Science and Technology Letters, 2019, 6, 696-701.	8.7	23
94	Toxicokinetics of benzo[a]pyrene in humans: Extensive metabolism as determined by UPLC-accelerator mass spectrometry following oral micro-dosing. Toxicology and Applied Pharmacology, 2019, 364, 97-105.	2.8	23
95	Phosphoproteomics Profiling of Human Skin Fibroblast Cells Reveals Pathways and Proteins Affected by Low Doses of Ionizing Radiation. PLoS ONE, 2010, 5, e14152.	2.5	21
96	Bioinformatics resource manager v2.3: an integrated software environment for systems biology with microRNA and cross-species analysis tools. BMC Bioinformatics, 2012, 13, 311.	2.6	21
97	Specific mutations in H5N1 mainly impact the magnitude and velocity of the host response in mice. BMC Systems Biology, 2013, 7, 69.	3.0	20
98	Genetic and Epigenetic Changes in Chromosomally Stable and Unstable Progeny of Irradiated Cells. PLoS ONE, 2014, 9, e107722.	2.5	19
99	Heterozygous variants in <i>MYBPC1</i> are associated with an expanded neuromuscular phenotype beyond arthrogryposis. Human Mutation, 2019, 40, 1115-1126.	2.5	19
100	Quantitative phosphoproteomics identifies filaggrin and other targets of ionizing radiation in a human skin model. Experimental Dermatology, 2012, 21, 352-357.	2.9	18
101	Diet-induced obesity reprograms the inflammatory response of the murine lung to inhaled endotoxin. Toxicology and Applied Pharmacology, 2013, 267, 137-148.	2.8	18
102	The Role of EGFR in Influenza Pathogenicity: Multiple Network-Based Approaches to Identify a Key Regulator of Non-lethal Infections. Frontiers in Cell and Developmental Biology, 2019, 7, 200.	3.7	18
103	Cell typeâ€dependent gene transcription profile in a threeâ€dimensional human skin tissue model exposed to low doses of ionizing radiation: Implications for medical exposures. Environmental and Molecular Mutagenesis, 2012, 53, 247-259.	2.2	17
104	Accumulation of CD11b+Gr-1+ cells in the lung, blood and bone marrow of mice infected with highly pathogenic H5N1 and H1N1 influenza viruses. Archives of Virology, 2013, 158, 1305-1322.	2.1	17
105	The multi-dimensional embryonic zebrafish platform predicts flame retardant bioactivity. Reproductive Toxicology, 2020, 96, 359-369.	2.9	17
106	Quantitative Phosphoproteome Analysis of Lysophosphatidic Acid Induced Chemotaxis Applying Dual-Step <sup>18</sup> 0 Labeling Coupled with Immobilized Metal-Ion Affinity Chromatography. Journal of Proteome Research, 2008, 7, 4215-4224.	3.7	16
107	Hepatic leukemia factor promotes resistance to cell death: Implications for therapeutics and chronotherapy. Toxicology and Applied Pharmacology, 2013, 268, 141-148.	2.8	16
108	Development of an environmental health tool linking chemical exposures, physical location and lung function. BMC Public Health, 2019, 19, 854.	2.9	16

#	Article	IF	CITATIONS
109	Unfolded Protein Response Inhibition Reduces Middle East Respiratory Syndrome Coronavirus-Induced Acute Lung Injury. MBio, 2021, 12, e0157221.	4.1	16
110	DNA microarray analysis reveals a role for lysophosphatidic acid in the regulation of anti-inflammatory genes in MC3T3-E1 cells. Bone, 2007, 41, 833-841.	2.9	15
111	A Community-Based Approach to Developing a Mobile Device for Measuring Ambient Air Exposure, Location, and Respiratory Health. Environmental Justice, 2015, 8, 126-134.	1.5	15
112	Cellular dichotomy between anchorageâ€independent growth responses to bFGF and TPA reflects molecular switch in commitment to carcinogenesis. Molecular Carcinogenesis, 2009, 48, 1059-1069.	2.7	14
113	Regulation of gene expression and subcellular protein distribution in MLO-Y4 osteocytic cells by lysophosphatidic acid: Relevance to dendrite outgrowth. Bone, 2011, 48, 1328-1335.	2.9	14
114	Quantitative proteomic analysis of mitochondrial proteins reveals prosurvival mechanisms in the perpetuation of radiation-induced genomic instability. Free Radical Biology and Medicine, 2012, 53, 618-628.	2.9	13
115	Sequential projection pursuit principal component analysis – dealing with missing data associated with new -omics technologies. BioTechniques, 2013, 54, 165-168.	1.8	13
116	ERK Oscillation-Dependent Gene Expression Patterns and Deregulation by Stress Response. Chemical Research in Toxicology, 2014, 27, 1496-1503.	3.3	13
117	Data integration reveals key homeostatic mechanisms following low dose radiation exposure. Toxicology and Applied Pharmacology, 2015, 285, 1-11.	2.8	13
118	A resource of lipidomics and metabolomics data from individuals with undiagnosed diseases. Scientific Data, 2021, 8, 114.	5.3	12
119	Early life stage trimethyltin exposure induces ADP-ribosylation factor expression and perturbs the vascular system in zebrafish. Toxicology, 2012, 302, 129-139.	4.2	11
120	The Effects of Low-Dose Irradiation on Inflammatory Response Proteins in a 3D Reconstituted Human Skin Tissue Model. Radiation Research, 2012, 178, 591-599.	1.5	11
121	Retinoic acidâ€dependent regulation of miRâ€19 expression elicits vertebrate axis defects. FASEB Journal, 2013, 27, 4866-4876.	0.5	11
122	Impaired Transcriptional Response of the Murine Heart to Cigarette Smoke in the Setting of High Fat Diet and Obesity. Chemical Research in Toxicology, 2013, 26, 1034-1042.	3.3	11
123	Influenza-Omics and the Host Response: Recent Advances and Future Prospects. Pathogens, 2017, 6, 25.	2.8	11
124	The landscape of viral proteomics and its potential to impact human health. Expert Review of Proteomics, 2016, 13, 579-591.	3.0	9
125	Evaluating predictive relationships between wristbands and urine for assessment of personal PAH exposure. Environment International, 2022, 163, 107226.	10.0	9
126	IgG4â€related disease: Association with a rare gene variant expressed in cytotoxic T cells. Molecular Genetics & Genomic Medicine, 2019, 7, e686.	1.2	8

#	Article	IF	CITATIONS
127	Time-dependent behavioral data from zebrafish reveals novel signatures of chemical toxicity using point of departure analysis. Computational Toxicology, 2019, 9, 50-60.	3.3	8
128	An Extensible, Scalable Architecture for Managing Bioinformatics Data and Analyses. , 2008, , .		7
129	An approach for calculating a confidence interval from a single aquatic sample for monitoring hydrophobic organic contaminants. Environmental Toxicology and Chemistry, 2012, 31, 2888-2892.	4.3	7
130	Proteomic analysis reveals down-regulation of surfactant protein B in murine type II pneumocytes infected with influenza A virus. Virology, 2015, 483, 96-107.	2.4	7
131	Dibenzo[ <i>def,p</i> ]chrysene transplacental carcinogenesis in wild-type, <i>Cyp1b1</i> knockout, and <i>CYP1B1</i> humanized mice. Molecular Carcinogenesis, 2017, 56, 163-171.	2.7	7
132	Unified feature association networks through integration of transcriptomic and proteomic data. PLoS Computational Biology, 2019, 15, e1007241.	3.2	7
133	Statistically Driven Metabolite and Lipid Profiling of Patients from the Undiagnosed Diseases Network. Analytical Chemistry, 2020, 92, 1796-1803.	6.5	7
134	The Ahr2-Dependent <i>wfikkn1</i> Gene Influences Zebrafish Transcriptome, Proteome, and Behavior. Toxicological Sciences, 2022, 187, 325-344.	3.1	7
135	Application of a fuzzy neural network model in predicting polycyclic aromatic hydrocarbon-mediated perturbations of the Cyp1b1 transcriptional regulatory network in mouse skin. Toxicology and Applied Pharmacology, 2013, 267, 192-199.	2.8	6
136	Quantitative Proteomic Profiling of Low-Dose Ionizing Radiation Effects in a Human Skin Model. Proteomes, 2014, 2, 382-398.	3.5	6
137	Magnetic Resonance Imaging characteristics in case of TOR1AIP1 muscular dystrophy. Clinical Imaging, 2019, 58, 108-113.	1.5	6
138	Gene co-expression network analysis in zebrafish reveals chemical class specific modules. BMC Genomics, 2021, 22, 658.	2.8	6
139	Bioinformatics Resource Manager: a systems biology web tool for microRNA and omics data integration. BMC Bioinformatics, 2019, 20, 255.	2.6	5
140	Atomic Force Microscopy and Infrared Nanospectroscopy of COVID-19 Spike Protein for the Quantification of Adhesion to Common Surfaces. Langmuir, 2021, 37, 12089-12097.	3.5	5
141	Direct detection of soil mRNAs using targeted microarrays for genes associated with lignin degradation. Soil Biology and Biochemistry, 2010, 42, 1793-1799.	8.8	4
142	Integration of Data Systems and Technology Improves Research and Collaboration for a Superfund Research Center. Journal of the Association for Laboratory Automation, 2012, 17, 275-283.	2.8	3
143	Bayesian Proteoform Modeling Improves Protein Quantification of Global Proteomic Measurements. Molecular and Cellular Proteomics, 2014, , .	3.8	3
144	P-Mart: Interactive Analysis of Ion Abundance Global Proteomics Data. Journal of Proteome Research, 2019, 18, 1426-1432.	3.7	3

#	Article	IF	CITATIONS
145	Expanding on Successful Concepts, Models, and Organization. Environmental Science & Technology, 2016, 50, 8921-8922.	10.0	1
146	Bayesian Posterior Integration for Classification of Mass Spectrometry Data. , 2017, , 203-211.		1
147	Analytics challengeHigh-throughput visual analytics biological sciences. , 2006, , .		0